JOURNAL OF MOLECULAR SPECTROSCOPY **108**, 17–30 (1984)

High Resolution Spectrum of the ν_5 Band of Nitric Acid (HNO_3) near 880 cm^{-1}

A. G. MAKI

Molecular Spectroscopy Division, National Bureau of Standards, Washington, D. C. 20234

AND

J. S. WELLS

Time and Frequency Division, National Bureau of Standards, Boulder, Colorado 80303

Tunable diode lasers have been used to measure the spectrum of HNO_3 from 853 to 892 cm^{-1}. A Fermi interaction with the nearby $2\nu_9$ state perturbs some of the transitions and causes some problems in the analysis, but several hundred lines have been assigned and fit to a set of band constants with a standard deviation of 0.0007 cm^{-1}. The measurements include most of the *P* branch, the strongest lines of the *Q* branch, and some *R*-branch transitions. Only *A*-type transitions have been identified and any *B*-type transitions must be much weaker.

I. INTRODUCTION

Nitric acid (HNO_3) is present in the upper atmosphere and is frequently measured by balloon or aircraft borne spectrometers (*1–3*) as well as from the ground (*4*). Interest in this atmospheric species stems from a need to monitor the concentration distribution of reactive species in order to understand the chemistry of the atmosphere and how it affects man (as well as how man affects it). The ν_5 band near 880 cm^{-1} is often used to monitor HNO_3 in the upper atmosphere and a thorough knowledge of the position, intensity, and assignment of the absorption lines is essential to a reliable analysis of the field measurements.

In this paper we are concerned with giving the position (frequency) and assignment of the strongest absorption features due to the ν_5 band. We also have some measurements of the line intensities which will be presented in a future paper dealing with the absorption intensity of the ν_5 band.

Chevillard and Giraudet (*5*) used a grille spectrometer to measure the low resolution spectrum of the ν_5 and $2\nu_9$ bands. Because of their limited resolution ($\sim$0.05 cm^{-1}), they were able to measure only the unresolved *P*- and *R*-branch clumps. They gave values for the band center and effective $\Delta\bar{B}$ and ΔC constants, but the most useful part of their paper was the spectrum that they published. Such a complete spectrum is very useful even though it may be of low resolution. One of the problems with assigning diode laser spectra is the lack of a compact, comprehensive overview of the entire system under study.

Brockman *et al.* (*6*) have published diode laser measurements on a portion of the *R*-branch region of ν_5 from 891 to 899 cm^{-1}. In two papers Dana (*7, 8*) has analyzed

0022-2852/84 $3.00

the measurements of both Brockman *et al.* (*6*) and Chevillard and Giraudet (*5*), and has given assignments for most of the strong features due to either the ν_5 band or the $2\nu_9$ band. The present work confirms some of Dana's assignments for the ν_5 band although there is disagreement on the assignment of many more of the transitions, particularly the *B*-type transitions which we believe are too weak to be observed.

II. EXPERIMENTAL DETAILS

The diode laser measurements were made in two different laboratories using two different diode laser elements and two different optical systems. The diode laser spectrometer used in the NBS–Washington laboratory was built by Terry Todd and Bruce Olson and has been briefly described by them (*9*). The diode laser spectrometer used in the NBS–Boulder laboratory is similar and was built by one of the authors (J.W.). The major difference between the two systems centers around the mode of calibration.

In all cases the calibration was provided by OCS absorption lines which were recorded at the same time that the HNO_3 absorption lines were recorded. In the NBS–Washington measurements the calibration lines were recorded by the same detector that recorded the HNO_3 spectrum. This was done by switching different absorption cells in and out of the laser beam at the appropriate moment as the spectrum was scanned. In the NBS–Boulder experiments the HNO_3 absorption cell could not be easily switched in and out of the beam; consequently a beam splitter was used to direct some of the laser radiation through the OCS absorption cell and onto a different detector than was used to record the HNO_3 spectrum. The NBS–Boulder experiments then recorded the fringe pattern from a solid germanium etalon in a succeeding scan in order to provide a wavenumber difference scale to be used to measure the wavenumber difference between the HNO_3 absorption lines and the OCS calibration lines. The NBS–Washington experiments recorded the germanium etalon fringes simultaneously with the spectral recording. In both cases solid germanium etalons 7.5 cm long were used. These had a free spectral range or interfringe separation of about 0.016 cm^{-1}. Although the technique used for the NBS–Washington measurements should be less prone to calibration errors, we have not been able to see any difference in the accuracy of the two techniques. The standard deviation of the fit of unperturbed lines was 0.0006 cm^{-1}.

The OCS calibration frequencies were taken from a listing being prepared by us for publication. These OCS calibration frequencies are based on heterodyne measurements given by Wells *et al.* (*10, 11*) and are generally accurate to ± 0.0001 cm^{-1}. We believe that the calibration errors will be randomly distributed throughout the band so that the uncertainties given by the least squares analysis of unperturbed transitions will reflect uncertainties in calibration as well as other measurement uncertainties or errors.

Several absorption cells were used for these measurements but the most recent measurements used absorption cells with BaF_2 windows which seem to be unaffected by the low pressures of HNO_3 used for these measurements, at least for the short times that the windows were exposed to the gas. The measurements were made with less than 1 Torr (133 Pa) HNO_3 and pathlengths that varied between 20 and 40 cm.

The observed transitions and their assignments are given in Table I. The next section describes how those assignments were made and what evidence supports those assignments.

III. DETAILS OF THE APPEARANCE AND ASSIGNMENTS OF THE BAND

Nitric acid is a planar oblate asymmetric rotor with C_s symmetry. According to McGraw *et al.* (*12*) the ν_5 band is an in-plane NO_2 deformation mode of symmetry species A'. Since it is an in-plane mode, it may give rise to a hybrid A-type and B-type band. For the A-type selection rules the strongest allowed transitions will be

$$\Delta J = 0, \pm 1; \qquad \Delta K_a = 0; \qquad \Delta K_c = \pm 1,$$

whereas the strongest allowed transitions for B-type selection rules will be

$$\Delta J = 0, \pm 1; \qquad \Delta K_a = \pm 1; \qquad \Delta K_c = \pm 1.$$

Since the A rotational axis (the axis of smallest moment of inertia) nearly bisects the NO_2 group, an NO_2 deformation vibration would be expected to give rise to a large change in the electric moment along the A axis and a small change along the B axis. Consequently, one would expect that ν_5 should be primarily an A-type band. On the other hand, Dana (*7*) has assigned a number of absorption lines to B-type transitions so the B-type selection rules must be considered in making the assignments.

The P-Branch and R-Branch Measurements

In an earlier paper (*13*) we described the appearance of a B-type band of HNO_3, the ν_2 band. A cursory examination of the P- and R-branch regions of the ν_5 band indicates that it looks quite similar. There is one minor but significant difference in the P- and R-branch region as described in the next paragraph.

In the analysis of the B-type ν_2 band a series of strong transitions was found with a spacing of 0.8 cm^{-1} ($2\bar{B}$). This series was due to P- and R-branch transitions of the unresolved doublet from states given by $J'' = K''_a$ and $K''_c = 0$ or 1. Trial calculations have shown that these lines are quite strong in B-type bands for HNO_3, but have only a very low intensity in A-type bands. Although there are a number of fairly strong unassigned transitions in our diode spectra, we were not able to identify any transitions of this type, even when we were able to calculate these transitions fairly reliably. This was our first strong indication that the B-type transitions must be weak for the ν_5 band.

The spectrum of the ν_5 band in the P- and R-branch regions consists of clumps of lines with a spacing of 0.4 cm^{-1} between clumps. Within each clump there is a regular series of lines coming to a head at the low frequency side of the clump. These clumps look very much like those shown in Fig. 2 of Ref. (*13*) except that all the lines are well separated. The series of lines within each clump is well ordered in the regions far from the band center (i.e., from 853 to 863 cm^{-1}) but the order within the clumps breaks down at several places. Calculated spectra show that this breakdown in the ordered series within each clump can not be attributed to the onset of the asymmetry splitting. It must be due to a perturbation that affects some of the energy levels of the ν_5 band.

TABLE I

Wavenumbers and Assignments of Measured HNO_3 Absorption Lines from 853 to 892 cm^{-1} [a]

TRANSITION J' KA'KC'			J" KA"KC"			MEASURED WAVENUMBER[a] (CM^{-1})	O - C (CM^{-1})
56	0	56 -	57	0	57	853.0964	0.0000
55	1	54 -	56	1	55	853.1325*	-0.0022
54	2	52 -	55	2	53	853.1647	-0.0011
53	3	50 -	54	3	51	853.1920	0.0000
51	5	46 -	52	5	47	853.2386	0.0019
50	6	44 -	51	6	45	853.2591	0.0010
49	7	42 -	50	7	43	853.2789	-0.0011
48	8	40 -	49	8	41	853.2989*	-0.0044
47	9	38 -	48	9	39	853.3194*	-0.0089
46	10	36 -	47	10	37	853.3414*	-0.0139
40	4	36 -	41	4	37	858.9405	-0.0007
39	5	34 -	40	5	35	858.9586	-0.0012
38	6	32 -	39	6	33	858.9776	-0.0017
37	7	30 -	38	7	31	858.9979	-0.0020
36	8	28 -	37	8	29	859.0225	0.0006
43	0	43 -	44	0	44	859.3366	0.0009
42	1	41 -	43	1	42	859.3566	0.0001
41	2	39 -	42	2	40	859.3755	0.0003
40	3	37 -	41	3	38	859.3932	0.0001
39	4	35 -	40	4	36	859.4106	-0.0003
38	5	33 -	39	5	34	859.4283	-0.0009
37	6	31 -	38	6	32	859.4470	-0.0015
36	7	29 -	37	7	30	859.4677	-0.0012
35	8	27 -	36	8	28	859.4920	0.0014
34	9	25 -	35	9	26	859.5224*	0.0088
42	0	42 -	43	0	43	859.8077	0.0007
41	1	40 -	42	1	41	859.8270	0.0003
40	2	38 -	41	2	39	859.8445	-0.0003
39	3	36 -	40	3	37	859.8619	-0.0002
38	4	34 -	39	4	35	859.8791	-0.0004
37	5	32 -	38	5	33	859.8963	-0.0012
36	6	30 -	37	6	31	859.9154	-0.0011
35	7	28 -	36	7	29	859.9372	0.0006
34	8	26 -	35	8	27	859.9632*	0.0051
41	0	41 -	42	0	42	860.2773	0.0003
40	1	39 -	41	1	40	860.2959	0.0001
39	2	37 -	40	2	38	860.3132	0.0001
38	3	35 -	39	3	36	860.3299	-0.0001
37	4	33 -	38	4	34	860.3467	-0.0003
36	5	31 -	37	5	32	860.3642	-0.0004
35	6	29 -	36	6	30	860.3826	-0.0007
34	7	27 -	35	7	28	860.4045	0.0013
33	8	25 -	34	8	26	860.4315*	0.0071
40	0	40 -	41	0	41	860.7458	0.0000
39	1	38 -	40	1	39	860.7637	0.0001
38	2	36 -	39	2	37	860.7805	0.0002
37	3	34 -	38	3	35	860.7966	0.0000
36	4	32 -	37	4	33	860.8129	-0.0003
35	5	30 -	36	5	31	860.8302	-0.0004
34	6	28 -	35	6	29	860.8495	0.0005
33	7	26 -	34	7	27	860.8719	0.0033
32	8	24 -	33	8	25	860.9010*	0.0115
38	0	38 -	39	0	39	861.6802	0.0006
37	1	36 -	38	1	37	861.6960	0.0003
36	2	34 -	37	2	35	861.7113	0.0002
35	3	32 -	36	3	33	861.7266	0.0002
34	4	30 -	35	4	31	861.7422	-0.0001
33	5	28 -	34	5	29	861.7605	0.0015
32	6	26 -	33	6	27	861.7812*	0.0044
31	7	24 -	32	7	25	861.8057*	0.0099
30	8	22 -	31	8	23	861.8474*	0.0314
37	0	37 -	38	0	38	862.1439	-0.0007
36	1	35 -	37	1	36	862.1594	-0.0005
35	2	33 -	36	2	34	862.1744	-0.0003
34	3	31 -	35	3	32	862.1896	0.0000
33	4	29 -	34	4	30	862.2049	-0.0001
32	5	27 -	33	5	28	862.2226	0.0012
31	6	25 -	32	6	26	862.2434*	0.0044
30	7	23 -	31	7	24	862.2726*	0.0149
36	0	36 -	37	0	37	862.6086*	0.0002
35	1	34 -	36	1	35	862.6229	0.0000
34	2	32 -	35	2	33	862.6374	0.0003
33	3	30 -	34	3	31	862.6517	0.0002
32	4	28 -	33	4	29	862.6671	0.0005
31	5	26 -	32	5	27	862.6846*	0.0019
30	6	24 -	31	6	25	862.7064*	0.0065
29	7	22 -	30	7	23	862.7408*	0.0225
35	0	35 -	36	0	36	863.0710	0.0001
34	1	33 -	35	1	34	863.0848	0.0001
33	2	31 -	34	2	32	863.0987	0.0004
32	3	29 -	33	3	30	863.1128	0.0005
31	4	27 -	32	4	28	863.1283	0.0012
30	5	25 -	31	5	26	863.1462*	0.0034
29	6	23 -	30	6	24	863.1704*	0.0107
28	7	21 -	29	7	22	863.2195*	0.0417
34	0	34 -	35	0	35	863.5316	-0.0006
33	1	32 -	34	1	33	863.5449	-0.0004
32	2	30 -	33	2	31	863.5584	0.0000
31	3	28 -	32	3	29	863.5723	0.0004
30	4	26 -	31	4	27	863.5879	0.0016
29	5	24 -	30	5	25	863.6068*	0.0051
32	0	32 -	33	0	33	864.4514	0.0004
31	1	30 -	32	1	31	864.4629*	0.0001
30	2	28 -	31	2	29	864.4750	0.0001
29	3	26 -	30	3	27	864.4882	0.0006
25	7	18 -	26	7	19	864.4961*	-0.0529
28	4	24 -	29	4	25	864.5038*	0.0026
27	5	22 -	28	5	23	864.5271*	0.0111
24	8	16 -	25	8	17	864.5325*	-0.0343
23	9	14 -	24	9	15	864.5551*	-0.0297
22	10	12 -	23	10	13	864.5739*	-0.0279
25	6	19 -	26	6	20	864.9025*	-0.0845
31	0	31 -	32	0	32	864.9083	-0.0003
30	1	29 -	31	1	30	864.9196	-0.0002
29	2	27 -	30	2	28	864.9313	0.0000
28	3	25 -	29	3	26	864.9447	0.0011
27	4	23 -	28	4	24	864.9615*	0.0046
24	7	17 -	25	7	18	864.9709*	-0.0327
26	5	21 -	27	5	22	864.9928*	0.0214
23	8	15 -	24	8	16	864.9928*	-0.0282
22	9	13 -	23	9	14	865.0110*	-0.0272
21	10	11 -	22	10	12	865.0302*	-0.0235
30	0	30 -	31	0	31	865.3645	-0.0004
29	1	28 -	30	1	29	865.3753	-0.0002
28	2	26 -	29	2	27	865.3868	0.0002
27	3	24 -	28	3	25	865.4002	0.0017
24	6	18 -	25	6	19	865.4059*	-0.0350
26	4	22 -	27	4	23	865.4184*	0.0069
23	7	16 -	24	7	17	865.4334*	-0.0237
22	8	14 -	23	8	15	865.4526*	-0.0213
25	5	20 -	26	5	21	865.4897*	0.0641
28	0	28 -	29	0	29	866.2734	-0.0004
27	1	26 -	28	1	27	866.2830	-0.0003
26	2	24 -	27	2	25	866.2944	0.0009
25	3	22 -	26	3	23	866.3082*	0.0035
23	5	18 -	24	5	19	866.3082*	-0.0222
22	6	16 -	23	6	17	866.3293*	-0.0157
21	7	14 -	22	7	15	866.3460*	-0.0144
24	4	20 -	25	4	21	866.3613*	0.0443
27	0	27 -	28	0	28	866.7261	-0.0003
26	1	25 -	27	1	26	866.7353	-0.0001
23	4	19 -	24	4	20	866.7391*	-0.0288
25	2	23 -	26	2	24	866.7460	0.0009
24	3	21 -	25	3	22	866.7626*	0.0066
22	5	17 -	23	5	18	866.7680*	-0.0131
21	6	15 -	22	6	16	866.7836*	-0.0117
20	7	13 -	21	7	14	866.7990*	-0.0111
19	8	11 -	20	8	12	866.8143*	-0.0103
26	0	26 -	27	0	27	867.1777	0.0000
25	1	24 -	26	1	25	867.1859	-0.0003
24	2	22 -	25	2	23	867.1969*	0.0013
22	4	18 -	23	4	19	867.2058*	-0.0119
21	5	16 -	22	5	17	867.2213*	-0.0092
23	3	20 -	24	3	21	367.2327*	0.0266

a) ASTERISKS INDICATE LINES THAT ARE PERTURBED OR BLENDED.

TABLE I—*Continued*

TRANSITION J' KA'KC' J" KA"KC"	MEASURED WAVENUMBER (CM^{-1})	O - C (CM^{-1})	TRANSITION J' KA'KC' J" KA"KC"	MEASURED WAVENUMBER (CM^{-1})	O - C (CM^{-1})
20 6 14 - 21 6 15	867.2340*	-0.0103	12 6 6 - 13 6 7	870.7879	-0.0001
25 0 25 - 26 0 26	867.6277	-0.0002	11 8 4 - 12 8 5	870.8088	0.0003
24 1 23 - 25 1 24	867.6357	-0.0002	16 0 16 - 17 0 17	871.6226	-0.0008
22 3 19 - 23 3 20	867.6419*	-0.0131	15 1 14 - 16 1 15	871.6277	-0.0003
23 2 21 - 24 2 22	867.6470*	0.0022	14 2 12 - 15 2 13	871.6344	0.0004
21 4 17 - 22 4 18	867.6592*	-0.0071	10 6 4 - 11 6 5	871.6344*	0.0028
20 5 15 - 21 5 16	867.6716*	-0.0072	13 3 10 - 14 3 11	871.6408	-0.0005
19 6 13 - 20 6 14	867.6847*	-0.0075	12 4 8 - 13 4 9	871.6491	-0.0002
18 7 11 - 19 7 12	867.6979*	-0.0078	11 5 6 - 12 5 7	871.6558	-0.0002
17 8 9 - 18 8 10	867.7097*	-0.0079	10 7 4 - 11 7 5	871.6684	0.0003
24 0 24 - 25 0 25	868.0765	-0.0002	15 0 15 - 16 0 16	872.0610	-0.0002
23 1 22 - 24 1 23	868.0843	0.0000	14 1 13 - 15 1 14	872.0659	0.0004
21 3 18 - 22 3 19	868.0974*	-0.0053	13 2 11 - 14 2 12	872.0713	0.0001
22 2 20 - 23 2 21	868.1035*	0.0106	12 3 9 - 13 3 10	872.0782	0.0001
20 4 16 - 21 4 17	868.1084*	-0.0053	11 4 7 - 12 4 8	872.0858	0.0002
19 5 14 - 20 5 15	868.1202*	-0.0056	12 2 10 - 13 2 11	872.5054*	-0.0018
18 6 12 - 19 6 13	868.1324*	-0.0063	13 0 13 - 14 0 14	872.9329	-0.0002
17 7 10 - 18 7 11	868.1450*	-0.0065	12 1 11 - 13 1 12	872.9366*	-0.0002
16 8 8 - 17 8 9	868.1549*	-0.0064	11 2 9 - 12 2 10	872.9418	-0.0002
23 0 23 - 24 0 24	868.5238	-0.0006	10 3 7 - 11 3 8	872.9479	-0.0002
22 1 21 - 23 1 22	868.5315	0.0000	9 4 5 - 10 4 6	872.9512	-0.0017
21 2 19 - 22 2 20	868.5358*	-0.0040	12 0 12 - 13 0 13	873.3680	0.0008
20 3 17 - 21 3 18	868.5460*	-0.0032	11 1 10 - 12 1 11	873.3719	0.0012
19 4 15 - 20 4 16	868.5560*	-0.0039	10 2 8 - 11 2 9	873.3767	0.0012
18 5 13 - 19 5 14	868.5674*	-0.0043	9 3 6 - 10 3 7	873.3819	0.0008
17 6 11 - 18 6 12	868.5791*	-0.0049	8 4 4 - 9 4 5	873.3819*	0.0016
16 7 9 - 17 7 10	868.5906*	-0.0051	8 5 4 - 9 5 5	873.3887	0.0016
15 8 7 - 16 8 8	868.5972*	-0.0049	10 0 10 - 11 0 11	874.2327	0.0009
22 0 22 - 23 0 23	868.9700	-0.0008	9 1 8 - 10 1 9	874.2356	0.0009
21 1 20 - 22 1 21	868.9777	0.0002	8 2 6 - 9 2 7	874.2402	0.0013
20 2 18 - 21 2 19	868.9841*	-0.0013	7 3 4 - 8 3 5	874.2422*	0.0009
19 3 16 - 20 3 17	868.9922*	-0.0024	7 4 4 - 8 4 5	874.2443	0.0007
18 4 14 - 19 4 15	869.0019*	-0.0030	8 0 8 - 9 0 9	875.0914	-0.0001
17 5 12 - 18 5 13	869.0127*	-0.0036	7 0 7 - 8 0 8	875.5200	0.0005
16 6 10 - 17 6 11	869.0241*	-0.0039	5 0 5 - 6 0 6	876.3723	0.0005
15 7 8 - 16 7 9	869.0337*	-0.0045	4 0 4 - 5 0 5	876.7964	0.0003
21 0 21 - 22 0 22	869.4151	-0.0009	25 23 2 - 25 23 3	878.6376	0.0002
20 1 19 - 21 1 20	869.4219	-0.0004	25 23 3 - 25 23 2	878.6376	0.0009
19 2 17 - 20 2 18	869.4284*	-0.0015	30 29 2 - 30 29 1	878.6412*	-0.0009
18 3 15 - 19 3 16	869.4365*	-0.0022	29 28 1 - 29 28 2	878.6670	-0.0003
17 4 13 - 18 4 14	869.4458*	-0.0029	37 37 0 - 37 37 1	878.6708	-0.0001
16 5 11 - 17 5 12	869.4562*	-0.0035	36 36 0 - 36 36 1	878.6921	-0.0004
15 6 9 - 16 6 10	869.4678*	-0.0028	28 27 1 - 28 27 2	878.6921	0.0003
14 7 7 - 15 7 8	869.4759*	-0.0027	23 21 2 - 23 21 3	878.6921	-0.0005
12 8 4 - 13 8 5	869.8196*	-0.0041	22 20 3 - 22 20 2	878.7142	-0.0010
20 0 20 - 21 0 21	869.8599	0.0000	27 26 1 - 27 26 2	878.7142	-0.0013
19 1 18 - 20 1 19	869.8660	0.0001	35 35 0 - 35 35 1	878.7142	0.0006
18 2 16 - 19 2 17	869.8730	-0.0001	34 34 0 - 34 34 1	878.7339	-0.0003
17 3 14 - 18 3 15	869.8806*	-0.0010	26 25 2 - 26 25 1	878.7392	0.0007
16 4 12 - 17 4 13	869.8902*	-0.0011	21 19 2 - 21 19 3	878.7456	-0.0001
15 5 10 - 16 5 11	869.9001*	-0.0017	33 33 0 - 33 33 1	878.7550	0.0009
14 6 8 - 15 6 9	869.9096	-0.0021	20 18 3 - 20 18 2	878.7580	-0.0015
13 7 6 - 14 7 7	869.9156	0.0002	25 24 2 - 25 24 1	878.7614	0.0007
13 8 6 - 14 8 7	869.9156	-0.0016	32 32 0 - 32 32 1	878.7732	-0.0003
12 9 4 - 13 9 5	869.9506	-0.0011	20 18 2 - 20 18 3	878.7732	0.0007
11 8 3 - 12 8 4	870.1568*	-0.0022	21 20 1 - 21 20 2	878.8428	0.0002
19 0 19 - 20 0 20	870.3021	-0.0005	8 7 2 - 8 7 1	878.8447*	0.0011
18 1 17 - 19 1 18	870.3078	-0.0004	28 28 0 - 28 28 1	878.8447*	-0.0008
17 2 15 - 18 2 16	870.3145	-0.0006	27 27 0 - 27 27 1	878.8618	-0.0002
16 3 13 - 17 3 14	870.3222*	-0.0011	20 19 1 - 20 19 2	878.8618	0.0005
15 4 11 - 16 4 12	870.3315	-0.0012	26 26 0 - 26 26 1	878.8781	0.0001
14 5 9 - 15 5 10	870.3409*	-0.0017	19 18 1 - 19 18 2	878.8791	-0.0004
12 7 5 - 13 7 6	870.3409*	-0.0017	9 8 2 - 9 8 1	878.8908*	0.0000
13 6 7 - 14 6 8	870.3492	-0.0019	25 25 0 - 25 25 1	878.8931	-0.0003
12 8 5 - 13 8 6	870.3544	-0.0013	18 17 1 - 18 17 2	878.8973	0.0001
11 7 4 - 12 7 5	870.7354	-0.0013	24 24 0 - 24 24 1	878.9080	-0.0003
18 0 18 - 19 0 19	870.7443	0.0002	16 14 2 - 16 14 3	878.9080	-0.0001
17 1 16 - 18 1 17	870.7502	0.0008	1 1 1 - 1 1 0	878.9115	-0.0011
16 2 14 - 17 2 15	870.7564	0.0004	17 16 1 - 17 16 2	878.9145	-0.0001
15 3 12 - 16 3 13	870.7639	0.0000	23 23 0 - 23 23 1	878.9226	0.0000
14 4 10 - 15 4 11	870.7726	-0.0002	10 9 2 - 10 9 1	878.9258	0.0013
13 5 8 - 14 5 9	870.7818	-0.0002	16 15 1 - 16 15 2	878.9323	0.0004

TABLE I—*Continued*

TRANSITION J' KA'KC' - J" KA"KC"	MEASURED WAVENUMBER (CM^{-1})	O - C (CM^{-1})	TRANSITION J' KA'KC' - J" KA"KC"	MEASURED WAVENUMBER (CM^{-1})	O - C (CM^{-1})
22 22 0 - 22 22 1	878.9363	0.0000	11 1 10 - 10 1 9	884.2325	-0.0002
2 2 1 - 2 2 0	878.9363	-0.0009	10 2 8 - 9 2 7	884.2396	-0.0005
15 14 2 - 15 14 1	878.9382	0.0003	9 3 6 - 8 3 5	884.2500	0.0002
11 10 2 - 11 10 1	878.9448	0.0002	13 0 13 - 12 0 12	884.6277	-0.0002
15 14 1 - 15 14 2	878.9496	-0.0002	12 1 11 - 11 1 10	884.6342	0.0002
14 13 2 - 14 13 1	878.9496*	0.0019	11 2 9 - 10 2 8	884.6424	0.0008
21 21 0 - 21 21 1	878.9496	0.0001	10 3 7 - 9 3 6	884.6515	0.0004
13 12 2 - 13 12 1	878.9539	0.0004	14 0 14 - 13 0 13	885.0270	-0.0007
12 11 2 - 12 11 1	878.9539	0.0006	13 1 12 - 12 1 11	885.0342	0.0002
20 20 0 - 20 20 1	878.9621	0.0000	12 2 10 - 11 2 9	885.0418	0.0000
15 13 2 - 15 13 3	878.9621	0.0006	11 3 8 - 10 3 7	885.0510	-0.0004
3 3 1 - 3 3 0	878.9695*	0.0013	10 4 6 - 9 4 5	885.0640	-0.0002
14 13 1 - 14 13 2	878.9695	0.0004	15 0 15 - 14 0 14	885.4251*	-0.0011
19 19 0 - 19 19 1	878.9748	0.0006	14 1 13 - 13 1 12	885.4327	-0.0001
18 18 0 - 18 18 1	878.9853	-0.0005	13 2 11 - 12 2 10	885.4409	0.0001
13 12 1 - 13 12 2	878.9910	-0.0001	12 3 9 - 11 3 8	885.4508	0.0003
17 17 0 - 17 17 1	878.9967	-0.0001	11 4 7 - 10 4 6	885.4638	0.0012
4 4 1 - 4 4 0	878.9993	-0.0004	21 0 21 - 20 0 20	887.7914	0.0008
16 16 0 - 16 16 1	879.0066	-0.0007	20 1 19 - 19 1 18	887.8004	0.0013
15 15 0 - 15 15 1	879.0172	-0.0001	19 2 17 - 18 2 16	887.8094*	0.0006
15 15 1 - 15 15 0	879.0172	0.0002	18 3 15 - 17 3 14	887.8201*	0.0003
12 11 1 - 12 11 2	879.0172	-0.0006	17 4 13 - 16 4 12	887.8320*	-0.0003
14 14 1 - 14 14 0	879.0262	-0.0001	16 5 11 - 15 5 10	887.8459*	-0.0006
14 14 0 - 14 14 1	879.0262	-0.0007	22 0 22 - 21 0 21	888.1774*	-0.0028
5 5 1 - 5 5 0	879.0262	0.0001	21 1 20 - 20 1 19	888.1874	-0.0017
13 13 1 - 13 13 0	879.0358	0.0008	20 2 18 - 19 2 17	888.1962*	-0.0029
13 13 0 - 13 13 1	879.0358	-0.0003	19 3 16 - 18 3 15	888.2074*	-0.0030
11 10 1 - 11 10 2	879.0516	-0.0003	18 4 14 - 17 4 13	888.2190*	-0.0041
11 11 0 - 11 11 1	879.0547	0.0007	17 5 12 - 16 5 11	888.2331*	-0.0043
10 10 1 - 10 10 0	879.0547	-0.0006	23 0 23 - 22 0 22	888.5680	-0.0005
7 7 1 - 7 7 0	879.0547	-0.0005	22 1 21 - 21 1 20	888.5777	-0.0002
8 8 1 - 8 8 0	879.0591	-0.0002	21 2 19 - 20 2 18	888.5844*	-0.0038
9 9 1 - 9 9 0	879.0591	0.0003	20 3 17 - 19 3 16	888.5969*	-0.0028
10 10 0 - 10 10 1	879.0628	-0.0004	19 4 15 - 18 4 14	888.6098*	-0.0028
9 9 0 - 9 9 1	879.0742	0.0007	31 0 31 - 30 0 30	891.6275	-0.0011
8 8 0 - 8 8 1	879.0857	-0.0002	25 6 19 - 24 6 18	891.6325*	-0.0858
10 9 1 - 10 9 2	879.0973	0.0005	30 1 29 - 29 1 28	891.6408	-0.0011
7 7 0 - 7 7 1	879.1026	0.0007	29 2 27 - 28 2 26	891.6548	-0.0006
13 11 2 - 13 11 3	879.1148*	-0.0023	28 3 25 - 27 3 24	891.6696	0.0001
6 6 0 - 6 6 1	879.1231	-0.0004	27 4 23 - 26 4 22	891.6878*	0.0033
5 5 0 - 5 5 1	879.1541*	0.0015	24 7 17 - 23 7 16	891.7033*	-0.0342
9 8 1 - 9 8 2	879.1541	-0.0008	26 5 21 - 25 5 20	891.7202*	0.0195
4 4 0 - 4 4 1	879.1890	-0.0002	23 8 15 - 22 8 14	891.7307*	-0.0277
12 10 2 - 12 10 3	879.2211*	-0.0024	22 9 13 - 21 9 12	891.7556*	-0.0257
8 7 1 - 8 7 2	879.2269	-0.0002	21 10 11 - 20 10 10	891.7834*	-0.0240
3 3 0 - 3 3 1	879.2304	0.0001	26 6 20 - 25 6 19	892.0000*	-0.0972
2 2 0 - 2 2 1	879.2692	-0.0007	31 1 30 - 30 1 29	892.0181	-0.0011
1 1 0 - 1 1 1	879.3012	0.0003	30 2 28 - 29 2 27	892.0329	-0.0002
7 6 1 - 7 6 2	879.3100	-0.0003	29 3 26 - 28 3 25	892.0483	0.0007
11 9 2 - 11 9 3	879.3447	-0.0014	25 7 18 - 24 7 17	892.0636*	-0.0529
6 5 1 - 6 5 2	879.3998	0.0009	27 5 22 - 26 5 21	892.0919*	0.0125
10 8 2 - 10 8 3	879.4796	0.0007	24 8 16 - 23 8 15	892.1049*	-0.0326
5 4 1 - 5 4 2	879.4861	0.0003	23 9 14 - 22 9 13	892.1323*	-0.0281
4 3 1 - 4 3 2	879.5658	0.0008	22 10 12 - 21 10 11	892.1597*	-0.0262
9 7 2 - 9 7 3	879.6142	0.0001	33 0 33 - 32 0 32	892.3806	0.0000
3 2 1 - 3 2 2	879.6318	-0.0003	32 1 31 - 31 1 30	892.3958	0.0007
2 1 1 - 2 1 2	879.6837	-0.0004	31 2 29 - 30 2 28	892.4102	0.0006
8 6 2 - 8 6 3	879.7434	-0.0006	30 3 27 - 29 3 26	892.4255	0.0011
7 5 2 - 7 5 3	879.8638	0.0017	29 4 25 - 28 4 24	892.4435*	0.0035
12 0 12 - 11 0 11	884.2266	-0.0003	28 5 23 - 27 5 22	892.4659*	0.0091

According to the assignments of McGraw *et al.* (*12*) there is only one vibrational state that is close enough to significantly perturb the ν_5 energy levels. That is the $2\nu_9$ state which is an A' state. A Fermi resonance interaction term will couple these two states but the 17-cm^{-1} separation of the ν_5 and $2\nu_9$ bands indicates that the bands can not be displaced by more than 8.5 cm^{-1}. There may also be a weak K-dependent Coriolis interaction coupling the ν_5 and $2\nu_9$ states, but much (and perhaps all) of the perturbation can be explained by the Fermi resonance.

The Fermi resonance can only couple levels with the same J and K values occurring in the same Wang factored energy matrix. However, the asymmetry matrix elements couple the levels J, K with J, $K \pm 2$. Thus the asymmetry mixes the different K levels in a given Wang symmetry block so that each level has a wavefunction that is a linear combination of the wavefunctions of the other K levels within the Wang symmetry block. In this way the Fermi resonance will couple, for instance, $K_a = 2$, $K_c = J - 2$ of ν_5 with $K_a = 0$, $K_c = J$ of $2\nu_9$.

Since the $2\nu_9$ band has not been analyzed with sufficient accuracy, in spite of the beginning made by Dana (*8*), there is much that we do not understand about the perturbations of the ν_5 band. We can be certain, however, that for ν_5 the levels $K_a = 0$, $K_c = J$; $K_a = 1$, $K_c = J - 1$; $K_a = 1$, $K_c = J$; and $K_a = 2$, $K_c = J - 1$ do not come close to any levels of $2\nu_9$ and so must be free of significant perturbations. This means that the initial work of assigning and fitting the ν_5 band should concentrate on those levels.

For low values of K_a the assignment was straightforward. The pattern was the same as that found for the ν_2 band regardless of whether A-type or B-type selection rules are followed. Since there was some uncertainty about the position of the band center, combination-differences were calculated from measurements of a number of pairs of P- and R-branch lines and checked against the ground state combination-differences which are well determined by the microwave measurements of DeLucia *et al.* (*14, 15*). These combination-differences proved that the assignment was correct.

To determine how good the measurements are as well as to determine initial estimates of the upper state constants, the P- and R-branch measurements of the transitions to the unperturbed levels ($K'_a = 0$ or 1, $K'_c = J'$ and $K'_a = 1$ or 2, $K'_c = J' - 1$) were fit. The standard deviation of the fit was 0.0006 cm^{-1}.

As soon as the next higher values of $K'_a = 2$ or 3, $K_c = J - 2$ were added to the fit, it was obvious that some of the transitions were being affected by perturbations. The affected transitions lay in the region from $J' = 19$ to $J' = 25$ with two lines missing in the center of this region. A calculation of the energy levels using estimated constants for ν_5 and $2\nu_9$ showed that the $K_a = 2$ or 3, $K_c = J - 2$ levels of ν_5 approach and cross the $K_a = 0$ or 1, $K_c = J$ levels of $2\nu_9$ in this range of J values with the crossing occurring between $J = 21$ and $J = 22$. The missing lines were later located as the perturbation pattern became obvious. The upper left panel of Fig. 1 shows how the observed transitions are displaced from their calculated positions.

The calculated energy levels also showed that successive crossings for higher values of K_a would occur at successively higher J values. We have observed that the $K_a = 3$ or 4, $K_c = J - 3$ levels of ν_5 cross the $K_a = 1$ or 2, $K_c = J - 1$ levels of $2\nu_9$ between $J = 22$ and $J = 23$. We also find a crossing for $K_a = 4$ or 5, $K_c = J - 4$ between $J = 23$ and $J = 24$ and for $k_a = 5$ or 6, $K_c = J - 5$ between $J = 24$ and $J = 25$. Figure 1 also shows the deviations observed for these crossings. Each successively higher value of K_a is more strongly perturbed and the $K_a = 6$, 7, 8, and higher levels are more difficult to assign in the region where the absorption lines are displaced the most. A more quantitative analysis of this perturbation does not seem worthwhile until more measurements of the $2\nu_9$ transitions and a better analysis of that band are available.

For either A-type or B-type selection rules the P- and R-branch transitions that form clumps spaced by 0.4 cm^{-1} are composed of a series of unresolved doublets.

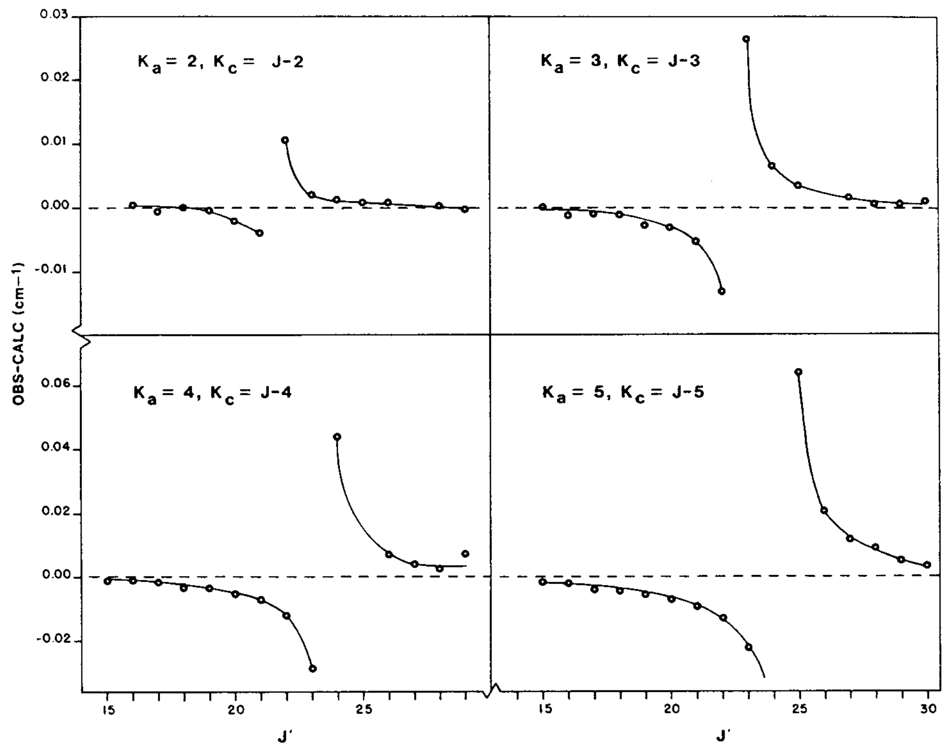

FIG. 1. Plots of deviations vs J' for some of the ν_5 transitions of HNO_3 that are perturbed by the Fermi resonance with $2\nu_9$. Note that the ordinate scale of the upper two plots is different from the ordinate scale of the lower two plots.

The lowest and strongest line of each series within a clump has the lower state rotational quantum numbers $J'' = N$, $K_a'' = 0$ or 1, $K_c'' = N$; the next line in the series will have $J'' = N - 1$, $K_a'' = 1$ or 2, $K_c'' = N - 2$, the next will have $J'' = N - 2$, $K_a'' = 2$ or 3, $K_c'' = N - 4$, etc. The difference between A-type and B-type selection rules can only be discerned for higher values of K_a where the asymmetry splitting is large enough in both the upper and lower levels to resolve the doublets. Because of the perturbation and overlapping with the $2\nu_9$ band at low J values, it is not possible to identify with confidence the asymmetry split transitions in the P- and R-branch regions. Table I only gives the assignments of one component of the unresolved doublets.

The Q-Branch Measurements

After the strong P- and R-branch transitions had been assigned and fit, the upper state ro-vibrational band constants were not very accurate since there still remained some strong correlations among the constants, e.g., between the A and B rotational constants. It was also possible to assign the P- and R-branch transitions to either A-

type or B-type selection rules. To break the correlation among the constants and to determine for certain whether A-type or B-type selection rules are dominant, it was necessary to measure and assign some Q-branch transitions.

For an A-type band the low values of K_c give the strongest and most distinctly patterned Q-branch transitions. At this point preliminary calculations of the Q-branch transitions were made using the band constants obtained from the P- and R-branch fits. Calculations were made for A-type transitions and for B-type transitions, but only the calculated A-type transitions resembled the strongest observed Q-branch features (see Fig. 2). The most prominent features of an A-type Q branch for ν_5 are several series of lines. All the lines in each series have the same value of K_c (actually two values for the high J unsplit doublets) and successive lines within a series have increasing values of J and K_a. The strongest series is $K_a = J$, $K_c = 0$ or 1 and the strongest line within the $K_c = 0$ or 1 series is the $J = 16$ line. The strongest lines are all doublets with two possible values of K_c but at low J values the doublets become widely split. Several different assignments were tried and it was apparent that only one assignment would properly match up with the already assigned P- and R-branch transitions. Although there is a great deal of overlap of the Q-branch transitions, there are enough isolated lines for low J values of the two series $K_a = J$, $K_c'' = 1$ and $K_a = J - 1$, $K_c'' = 2$ to give unambiguous proof that the present assignment is correct.

The Q-branch region of the $2\nu_9$ band bears a strong resemblance to the Q branch of ν_5 and it would appear that A-type transitions also predominate for the $2\nu_9$ band. This might be expected if the Fermi resonance and consequent intensity borrowing from ν_5 is responsible for much of the intensity of the $2\nu_9$ band.

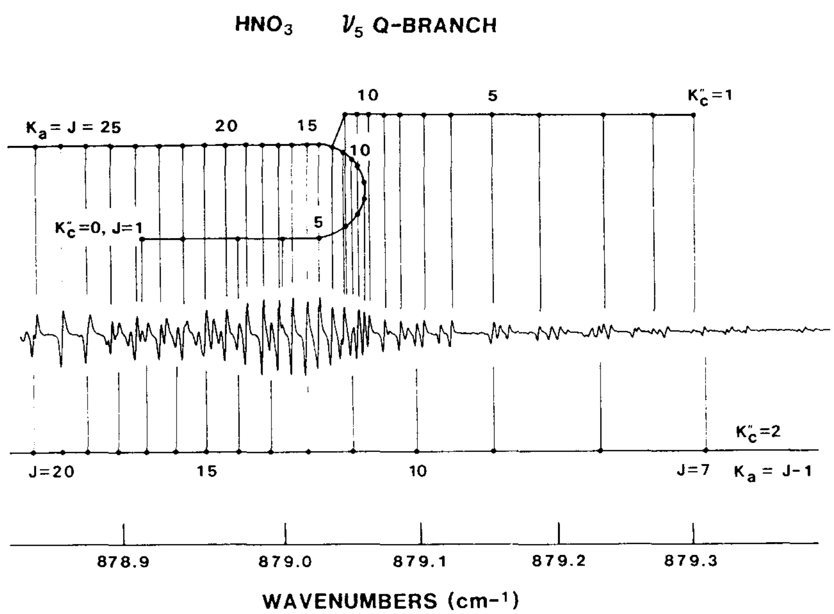

FIG. 2. The first-derivative spectrum of the Q-branch region of ν_5 of HNO_3. The $K_a = J$ transitions are identified above the spectrum and the $K_a = J - 1$ transitions for $K_c'' = 2$ are identified below the spectrum. All identified transitions are A-type Q-branch transitions.

TABLE II

Assignment and Recalibration of HNO_3 Transitions from 891 to 899 cm^{-1}

TRANSITION $J'\ K'_a\ K'_c - J''\ K''_a\ K''_c$	MEASURED WAVENUMBER (cm^{-1}) (REF. 6)	CALCULATED WAVENUMBER (cm^{-1})	TRANSITION $J'\ K'_a\ K'_c - J''\ K''_a\ K''_c$	MEASURED WAVENUMBER (cm^{-1}) (REF. 6)	CALCULATED WAVENUMBER (cm^{-1})
30 0 30 - 29 0 29	891.246	891.2507	36 3 33 - 35 3 32	894.666	894.659
29 1 28 - 28 1 27	891.258	891.2634	35 4 31 - 34 4 30	894.684	894.677
28 2 26 - 27 2 25	891.271	891.276	34 5 29 - 33 5 28	894.702	894.695
27 3 24 - 26 3 23	891.286	891.291	33 6 27 - 32 6 26	894.723	894.716
31 0 31 - 30 0 30	891.627	891.6286	32 7 25 - 31 7 24	894.748	894.741
30 1 29 - 29 1 28	891.641	891.6419	31 8 23 - 30 8 22	894.783	894.776
29 2 27 - 28 2 26	891.654	891.656	40 0 40 - 39 0 39	894.981	894.9709
28 3 25 - 27 3 24	891.669	891.670	39 1 38 - 38 1 37	895.001	894.9908
27 4 23 - 26 4 22	891.687	891.689	38 2 36 - 37 2 35	895.018	895.009
32 0 32 - 31 0 31	892.002	892.0053	37 3 34 - 36 3 33	895.036	895.027
31 1 30 - 30 1 29	892.017	892.0192	36 4 32 - 35 4 31	895.053	895.045
30 2 28 - 29 2 27	892.032	892.031	35 5 30 - 34 5 29	895.072	895.064
29 3 26 - 28 3 25	892.048	892.048	34 6 28 - 33 6 27	895.092	895.083
28 4 24 - 27 4 23	892.064	892.060	33 7 26 - 32 7 25	895.116	895.107
27 5 22 - 26 5 21	892.090	892.092	32 8 24 - 31 8 23	895.146	895.137
33 0 33 - 32 0 32	892.376	892.3806	41 0 41 - 40 0 40	895.340	895.3356
32 1 31 - 31 1 30	892.390	892.3951	40 1 39 - 39 1 38	895.361	895.3564
31 2 29 - 30 2 28	892.405	892.410	39 2 37 - 38 2 36	895.379	895.376
30 3 27 - 29 3 26	892.420	892.425	38 3 35 - 37 3 34	895.398	895.394
29 4 25 - 28 4 24	892.438	892.442	37 4 33 - 36 4 32	895.415	895.412
28 5 23 - 27 5 22	892.459	892.466	36 5 31 - 35 5 30	895.433	895.431
34 0 34 - 33 0 33	892.756	892.7546	35 6 29 - 34 6 28	895.454	895.451
33 1 32 - 32 1 31	892.775	892.7698	34 7 27 - 33 7 26	895.476	895.473
32 2 30 - 31 2 29	892.788	892.785	33 8 25 - 32 8 24	895.504	895.501
31 3 28 - 30 3 27	892.803	892.800	32 9 23 - 31 9 22	895.550	895.545
30 4 26 - 29 4 25	892.821	892.818	42 0 42 - 41 0 41	895.700	895.6990
29 5 24 - 28 5 23	892.842	892.838	41 1 40 - 40 1 39	895.720	895.7207
35 0 35 - 34 0 34	893.135	893.1273	40 2 38 - 39 2 37	895.741	895.740
34 1 33 - 33 1 32	893.150	893.1432	39 3 36 - 38 3 35	895.759	895.759
33 2 31 - 32 2 30	893.166	893.159	38 4 34 - 37 4 33	895.778	895.778
32 3 29 - 31 3 28	893.181	893.174	37 5 32 - 36 5 31	895.796	895.797
31 4 27 - 30 4 26	893.197	893.192	36 6 30 - 35 6 29	895.816	895.817
30 5 25 - 29 5 24	893.217	893.211	35 7 28 - 34 7 27	895.839	895.838
29 6 23 - 28 6 22	893.243	893.237	34 8 26 - 33 8 25	895.864	895.866
36 0 36 - 35 0 35	893.500	893.4987	33 9 24 - 32 9 23	895.899	895.900
35 1 34 - 34 1 33	893.517	893.5153	43 0 43 - 42 0 42	896.064	896.0610
34 2 32 - 33 2 31	893.533	893.531	42 1 41 - 41 1 40	896.083	896.0838
33 3 30 - 32 3 29	893.549	893.547	41 2 39 - 40 2 38	896.104	896.104
32 4 28 - 31 4 27	893.566	893.564	40 3 37 - 39 3 36	896.122	896.124
31 5 26 - 30 5 25	893.585	893.583	39 4 35 - 38 4 34	896.142	896.143
30 6 24 - 29 6 23	893.609	893.606	38 5 33 - 37 5 32	896.160	896.162
29 7 22 - 28 7 21	893.646	893.643	37 6 31 - 36 6 30	896.181	896.182
37 0 37 - 36 0 36	893.872	893.8687	36 7 29 - 35 7 28	896.203	896.203
36 1 35 - 35 1 34	893.889	893.8861	35 8 27 - 34 8 26	896.229	896.228
35 2 33 - 34 2 32	893.905	893.903	34 9 25 - 33 9 24	896.262	896.260
34 3 31 - 33 3 30	893.922	893.919	44 0 44 - 43 0 43	896.425	896.4217
33 4 29 - 32 4 28	893.939	893.936	43 1 42 - 42 1 41	896.448	896.4455
32 5 27 - 31 5 26	893.958	893.955	42 2 40 - 41 2 39	896.469	896.467
31 6 25 - 30 6 24	893.981	893.978	41 3 38 - 40 3 37	896.489	896.487
30 7 23 - 29 7 22	894.010	894.008	40 4 36 - 39 4 35	896.509	896.506
38 0 38 - 37 0 37	894.246	894.2374	39 5 34 - 38 5 33	896.528	896.526
37 1 36 - 36 1 35	894.265	894.2556	38 6 32 - 37 6 31	896.547	896.546
36 2 34 - 35 2 33	894.281	894.273	37 7 30 - 36 7 29	896.568	896.568
35 3 32 - 34 3 31	894.298	894.290	36 8 28 - 35 8 27	896.593	896.591
34 4 30 - 33 4 29	894.315	894.307	35 9 26 - 34 9 25	896.622	896.619
33 5 28 - 32 5 27	894.333	894.326	45 0 45 - 44 0 44	896.786	896.7811
32 6 26 - 31 6 25	894.355	894.348	44 1 43 - 43 1 42	896.809	896.8059
31 7 24 - 30 7 23	894.381	894.374	43 2 41 - 42 2 40	896.830	896.828
30 8 22 - 29 8 21	894.425	894.418	42 3 39 - 41 3 38	896.851	896.848
39 0 39 - 38 0 38	894.612	894.6048	41 4 37 - 40 4 36	896.871	896.868
38 1 37 - 37 1 36	894.631	894.6239	40 5 35 - 39 5 34	896.889	896.888
37 2 35 - 36 2 34	894.649	894.642	39 6 33 - 38 6 32	896.907	896.908

Analysis of Earlier Diode Data

Excellent diode laser measurements of the high *J* *R*-branch region of the ν_5 band have been published by Brockman *et al.* (*6*). While the absolute calibration of all

TABLE II-*Continued*

TRANSITION $J'\ K'_a\ K'_c\ -\ J''\ K''_a\ K''_c$	MEASURED WAVENUMBER (cm^{-1}) (REF. 6)	CALCULATED WAVENUMBER (cm^{-1})
38 7 31 - 37 7 30	896.928	896.930
37 8 29 - 36 8 28	896.951	896.953
36 9 27 - 35 9 26	896.978	896.979
35 10 25 - 34 10 24	897.008	897.010
46 0 46 - 45 0 45	897.139	897.1391
45 1 44 - 44 1 43	897.165	897.1651
44 2 42 - 43 2 41	897.189	897.188
43 3 40 - 41 3 39	897.211	897.209
42 4 38 - 41 4 37	897.231	897.229
41 5 36 - 40 5 35	897.250	897.249
40 6 34 - 39 6 33	897.269	897.270
39 7 32 - 38 7 31	897.289	897.292
38 8 30 - 37 8 29	897.312	897.315
37 9 28 - 36 9 27	897.338	897.341
36 10 26 - 35 10 25	897.373	897.372
47 0 47 - 46 0 46	897.504	897.4958
46 1 45 - 45 1 44	897.532	897.5229
45 2 43 - 44 2 42	897.554	897.546
44 3 41 - 43 3 40	897.576	897.568
43 4 39 - 42 4 38	897.597	897.588
42 5 37 - 41 5 36	897.615	897.609
41 6 35 - 40 6 34	897.635	897.630
40 7 33 - 39 7 32	897.656	897.652
39 8 31 - 38 8 30	897.680	897.675
38 9 29 - 37 9 28	897.705	897.700
37 10 27 - 36 10 26	897.735	897.729
48 0 48 - 47 0 47	897.862	897.8511
47 1 46 - 46 1 45	897.890	897.8795
46 2 44 - 45 2 43	897.913	897.904
45 3 42 - 44 3 41	897.935	897.926
44 4 40 - 43 4 39	897.956	897.947
43 5 38 - 42 5 37	897.976	897.967
42 6 36 - 41 6 35	897.995	897.988
41 7 34 - 40 7 33	898.014	898.011
40 8 32 - 39 8 31	898.037	898.034
39 9 30 - 38 9 29	898.060	898.059
38 10 28 - 37 10 27	898.089	898.086
37 11 26 - 36 11 25	898.125	898.122
49 0 49 - 48 0 48	898.212	898.2050
48 1 47 - 47 1 46	898.241	898.2347
47 2 45 - 46 2 44	898.261	898.260
46 3 43 - 45 3 42	898.289	898.283
45 4 41 - 44 4 40	898.310	898.304
44 5 39 - 43 5 38	898.330	898.325
43 6 37 - 42 6 36	898.350	898.346
42 7 35 - 41 7 34	898.369	898.368
41 8 33 - 40 8 32	898.392	898.392
40 9 31 - 39 9 30	898.416	898.417
39 10 29 - 38 10 28	898.444	898.444
38 11 27 - 37 11 26	898.478	898.477
50 0 50 - 49 0 49	898.567	898.5577
49 1 48 - 48 1 47	898.596	898.5887
48 2 46 - 47 2 45	898.623	898.615
47 3 44 - 46 3 43	898.648	898.638
46 4 42 - 45 4 41	898.669	898.660
45 5 40 - 44 5 39	898.689	898.681
44 6 38 - 43 6 37	898.708	898.702
43 7 36 - 42 7 35	898.729	898.724
42 8 34 - 41 8 33	898.750	898.748
41 9 32 - 40 9 31	898.773	898.773

those measurements is not quite as accurate as the present work, the relative line separations within an R-branch clump are more reliable. The region covered by the measurements of Brockman *et al.* includes the Q branch of $2\nu_9$ and many of the observed transitions must be due to the $2\nu_9$ band. Of course, there are also many hot band transitions amongst the ground state transitions.

One goal of the present work was to assign the ν_5 transitions that occur in the spectrum of Brockman *et al.* Table II lists those transitions which can be confidently assigned to the ν_5 band. Table II gives both the measured wavenumbers for the lines, as reported in Ref. (*6*), and the wavenumbers calculated for the lines as a result of the present work. We believe that our calculated values are more accurate than the measured values. In determining the calculated values we have made a crude adjustment for the effect of the resonance with $2\nu_9$. Since we believe that the calculated values are more reliable for the unperturbed subbands, the wavenumbers of those transitions are reported with four significant figures to the right of the decimal point whereas all other transitions are only reported with three digits to the right of the decimal point.

The line assignments given in Table II were based on the relative line intensities, and relative line spacings. The absolute frequency shift was assumed to be a slowly varying function of the measured frequency. The density of lines in this region is so great that it is always possible to find a line within 0.006 cm^{-1} of a predicted line, but we have required that the intensity of the R-branch regions, the appearance of the corresponding line in the *P*-branch region, and the intensity and frequency of nearby lines be consistent with the assignment.

IV. THE ROVIBRATIONAL CONSTANTS

We have fit the measurements given in Table I by using an improved version of the asymmetric rotor fitting program that was used in Ref. (*13*). The program was re-dimensioned to allow fitting data for higher *J* values. This program is based on Watson's *A*-reduced Hamiltonian in the prolate I^r, or oblate III^r or III^l representation (see Ref. (*17*)).

The ground state constants were determined in a separate fit of the microwave measurements given in Refs. (*14–16, 18, 19*).

For comparison with previous work we have fit the ground state data in the I^r, III^r, and III^l representations. The constants agree quite well with the values given by

TABLE III

Ground State Rotational Constants for HNO_3[a]

Constant	I^r Representation	III^r Representation
$A(cm^{-1})$	0.433999906 (44)	0.434001851(82)
$B(cm^{-1})$	0.403610064(40)	0.403608457(76)
$C(cm^{-1})$	0.208832488(28)	0.208832800(61)
$\Delta_J \times 10^6(cm^{-1})$	0.2971585(145)	0.4715020(1101)
$\Delta_{JK} \times 10^6(cm^{-1})$	-0.1516034(285)	-0.6730114(1086)
$\Delta_K \times 10^6(cm^{-1})$	0.2463635(345)	0.2461611(819)
$\delta_J \times 10^6(cm^{-1})$	0.12626554(547)	-0.03940715(641)
$\delta_K \times 10^6(cm^{-1})$	0.2493922(192)	0.6856705(1662)
$\Phi_J \times 10^{12}(cm^{-1})$	---	1.0077(427)
$\Phi_{JK} \times 10^{12}(cm^{-1})$	0.9127(176)	-3.4095(1285)
$\Phi_{KJ} \times 10^{12}(cm^{-1})$	-3.4609(665)	3.733(406)
$\Phi_K \times 10^{12}(cm^{-1})$	3.8081(514)	-1.304(275)
$\phi_J \times 10^{12}(cm^{-1})$	---	0.32631(229)
$\phi_{JK} \times 10^{12}(cm^{-1})$	---	4.3683(1044)
$\phi_K \times 10^{12}(cm^{-1})$	1.7508(273)	-35.088(1091)
σ(std. dev)(MHz)	0.1284	0.1580
number of transitions	242	242

a) The standard deviation is given in MHz in order to facilitate comparison with the fits given in Refs. (14, 15, and 16).

Bowman *et al.* (*15*), even though we included the data by Ghosh *et al.* (*16*), which was not available to Bowman *et al.* Both I^r and III^r constants are given in Table III. The I^r representation is less physically meaningful, but requires fewer constants to fit the data. The III^r representation seems to give more highly correlated constants than the I^r representation. All representations seem to fit the data equally well with nearly the same deviations.

To fit the upper state constants the ground state constants were fixed at the values determined by the microwave measurements. The infrared measurements were given a weight of either one or zero depending on how badly the lines were perturbed, or overlapped by other lines. The data given in Table II were not included in the least-squares fits.

It was difficult to decide which constants should be used in fitting this band. Because of the perturbation with $2\nu_9$ and because some levels of ν_5 are below all $2\nu_9$ levels and some levels are above some $2\nu_9$ levels with which they can interact, but below others, it is impossible to fit with a small number of constants all of the ν_5 transitions

TABLE IV

Upper State Rovibrational Constants for the ν_5 Band of HNO_3

	I^r Representation
$\nu_0(cm^{-1})$	879.10823(14)
$A'-A''(cm^{-1})$	-0.00022024(215)
$B'-B''(cm^{-1})$	-0.00190301(414)
$C'-C''(cm^{-1})$	-0.00061693(56)
$(\Delta'_J - \Delta''_J) \times 10^6(cm^{-1})$	-0.10888(1518)
$(\Delta'_{JK} - \Delta''_{JK}) \times 10^6(cm^{-1})$	0.5941(646)
$(\Delta'_K - \Delta''_K) \times 10^6(cm^{-1})$	-0.4781(500)
$(\delta'_J - \delta''_J) \times 10^6(cm^{-1})$	-0.05767(757)
$(\delta'_K - \delta''_K) \times 10^6(cm^{-1})$	0.17959(1167)
$(\Phi'_J - \Phi''_J) \times 10^{10}(cm^{-1})$	0.356(265)
$(\Phi'_{JK} - \Phi''_{JK}) \times 10^{10}(cm^{-1})$	-3.350(1597)
$(\Phi'_{KJ} - \Phi''_{KJ}) \times 10^{10}(cm^{-1})$	5.49(231)
$(\Phi'_K - \Phi''_K) \times 10^{10}(cm^{-1})$	-2.493(1077)
$(\phi'_J - \phi''_J) \times 10^{10}(cm^{-1})$	0.1754(1326)
$(\phi'_{JK} - \phi''_{JK}) \times 10^{10}(cm^{-1})$	-1.173(453)
$(\phi'_K - \phi''_K) \times 10^{10}(cm^{-1})$	2.015(432)
σ(std. dev) (cm^{-1})	0.0007
number of unperturbed transitions	273

to within the accuracy of the measurements. In Table IV we have given a set of constants that fits all but the most perturbed transitions with a standard deviation of ±0.0007 cm^{-1}. This standard deviation is only slightly larger than the accuracy of the measurements, but a few transitions with high values of J and K_0 show systematic deviations that are not due to errors in the measurements.

In Tables III and IV we have given the ground state constants used in these fits and the difference between the upper and lower state constants. The differences are given because they are not strongly correlated with the ground state constants. Because of the interaction with $2\nu_9$, the constants given in Table IV are only effective constants that can be used to calculate the transitions, but do not contain force field information for the ν_5 state. A more complete treatment of the Fermi resonance coupling the ν_5 and $2\nu_9$ states must await more high resolution measurements of the $2\nu_9$ band.

ACKNOWLEDGMENTS

One of the authors (A.M.) acknowledges the assistance of Wm. Bruce Olson who is responsible for the construction and continued operation of the diode laser system used in the NBS-Washington Laboratory. This work has been supported by the NASA Upper Atmospheric Research Office.

RECEIVED: May 16, 1983

REFERENCES

1. D. G. MURCRAY, T. G. KYLE, F. H. MURCRAY, AND W. J. WILLIAMS, *Nature London* **218,** 78–79 (1968).
2. D. G. MURCRAY, T. G. KYLE, F. H. MURCRAY, AND W. J. WILLIAMS, *J. Opt. Soc. Amer.* **59,** 1131–1134 (1969).
3. J.-C. FONTANELLA, A. GIRARD, L. FRAMONT, AND N. LOUISNARD, *Appl. Opt.* **14,** 825–839 (1975).
4. E. VIGROUX, *Pure Appl. Geophys.* **106,** 1336–1340 (1973).
5. J.-P. CHEVILLARD AND R. GIRAUDET, *J. Phys. Orsay Fr.* **39,** 517–520 (1978).
6. D. BROCKMAN, C. H. BAIR, AND F. ALLARIO, *Appl. Opt.* **17,** 91–100 (1978).
7. V. DANA, *Spectrochim. Acta Part A* **34,** 1027–1031 (1978).
8. V. DANA, *Spectrochim. Acta Part A* **37,** 421–423 (1981).
9. T. R. TODD AND W. B. OLSON, *J. Mol. Spectrosc.* **74,** 190–202 (1979).
10. J. S. WELLS, F. R. PETERSEN, A. G. MAKI, AND D. J. SUKLE, *Appl. Opt.* **20,** 1676–1684 (1981) and *Appl. Opt.* **20,** 2874 (1981).
11. J. S. WELLS, F. R. PETERSEN, A. G. MAKI, AND D. J. SUKLE, *J. Mol. Spectrosc.* **89,** 412–429 (1981).
12. G. E. MCGRAW, D. L. BERNITT, AND I. C. HISATSUNE, *J. Chem. Phys.* **42,** 237–244 (1965).
13. A. G. MAKI AND J. S. WELLS, *J. Mol. Spectrosc.* **82,** 427–434 (1980).
14. G. CAZZOLI AND F. C. DELUCIA, *J. Mol. Spectrosc.* **76,** 131–141 (1979).
15. W. C. BOWMAN, P. HELMINGER, AND F. C. DELUCIA, *J. Mol. Spectrosc.* **88,** 431–433 (1981).
16. P. N. GHOSH, C. E. BLOM, AND A. BAUDER, *J. Mol. Spectrosc.* **89,** 159–173 (1981).
17. J. K. G. WATSON, *in* "Vibrational Spectra and Structure, A Series of Advances," (J. R. Durig, Ed.), Vol. 6, Chap. I, Elsevier Scientific, New York, 1977.
18. D. J. MILLER AND J. R. MORTON, *Chem. Ind.* 945–954 (1956).
19. D. J. MILLER AND J. R. MORTON, *J. Chem. Soc.* 1523–1528 (1960).